

Investigation of peat sediments from Daiyun Mountain in southeast China: late Holocene vegetation, climate and human impact

Lin Zhao¹ · Chunmei Ma^{1,2} · Lingyu Tang³ · Kam-biu Liu⁴ · Limi Mao³ · Yu Zhang¹ · Huayu Lu¹ · Shuangye Wu^{1,5} · Qingyun Tu⁶

Received: 4 June 2015 / Accepted: 13 January 2016 / Published online: 3 February 2016
© Springer-Verlag Berlin Heidelberg 2016

Abstract In this study, late Holocene vegetation, climate and human impacts were investigated using multiproxy data—pollen percentages, pollen accumulation rates (PAR), humification and loss-on-ignition (LOI)—measured from peat sediments from Daiyun Mountain, southeast China. A stratigraphic chronology was established on the basis of four radiocarbon dates. The 4,350 year sequence of vegetation history and climate change exhibits three distinctive stages: (1) 4,350–1,000 cal BP, during which the vegetation was dominated by evergreen forests mainly composed of broad-leaf trees, indicating a warm and wet climate; (2) 1,000–550 cal BP, during which the climate was thought to be cool and dry, based on a decrease in pollen percentages and the PARs of trees, shrubs and wetland herbs, and an increase in the pollen percentage and PAR of dry land herbs, as well as high overall LOI values; and (3) 550 cal

BP to modern times, during which higher pollen percentages of dry land and wetland herbs, along with low pollen percentage and PAR of trees and shrubs, as well as low absorbance and LOI values, suggest relatively cooler but wetter climate conditions. In addition, major climatic events, such as the warm period from AD 670–960, the Medieval Warm Period (AD 1050–1520) and the Little Ice Age (AD 1580–1850), could be identified within the peat sediments in this study, with climatic conditions at these times being characteristically warm and wet, warm and dry, and cold and wet, respectively. Pollen signals indicate significant human impact since 1,000 cal BP, which may be linked to the development of the local porcelain industry and a rapid increase in the population in the study region.

Keywords Late holocene · Vegetation · Climate change · Human impact · Peat · Daiyun Mountain

Communicated by Y. Zhao.

✉ Chunmei Ma
chunmeima@nju.edu.cn

¹ School of Geographic and Oceanographic Sciences, Nanjing University, Nanjing 210023, China

² Jiangsu Collaborative Innovation Center for Climate Change, Nanjing 210093, China

³ State Key Laboratory of Palaeobiology and Stratigraphy, Nanjing Institute of Geology and Palaeontology, CAS, Nanjing 210008, China

⁴ Department of Oceanography and Coastal Sciences, School of the Coast and Environment, Louisiana State University, Baton Rouge, LA 70803, USA

⁵ Department of Geology, University of Dayton, 300 College Park, Dayton, OH 45469, USA

⁶ Daiyun Mountain National Nature Reserve Administration Bureau, Dehua 362503, Fujian, China

Introduction

Vegetation-based palaeoclimatic reconstruction can be used as a valuable input for modelling future global climate change. However, human interventions and influences on both vegetation and climate in the late Holocene can result in uncertainties in such modelling efforts. Owing to increasing interest in this field, several recent studies have focused on the vegetation and climate changes that occurred during the late Holocene, and particularly the influence of human activities on vegetation changes (Liu and Qiu 1994; Faust et al. 2004; van der Linden et al. 2008; Xu and Zhang 2013; Li et al. 2014; Turner et al. 2014; Cichon and Niedzielski 2015; Tian et al. 2015). Additionally, some authors have reported significant climate and environmental changes during the medieval warm period

(MWP) and the little ice age (LIA) (Chu et al. 2002; Cronin et al. 2003; Driese et al. 2004; Tan et al. 2009; Zeng et al. 2012; Quamar and Chauhan 2014; Sadori et al. 2015). Mountain peat sediments in particular are capable of preserving evidence of vegetation and climate change history, including the events such as the MWP and LIA (Viau et al. 2012; Zhang et al. 2014; Chen et al. 2015). Thus, studies into the dynamic vegetation landscape and contemporary climate conditions based on multiple proxy data from mountain peat sediments can be considered as critically important for understanding the late Holocene palaeoenvironment.

Southeastern subtropical China lies directly in the path of the summer monsoon circulation, and is a key region for the study of monsoon variability and vegetation reconstruction during the late Quaternary. Daiyun Mountain, in Fujian Province, is located in this subtropical region of southeastern China, and is significantly affected by monsoon changes. As such, the changing East Asian Monsoon climate may be recorded as vegetation changes upon Daiyun Mountain, and therefore reconstruction of the palaeovegetation of this region is of great importance. The peat sediments of Daiyun Mountain are predominantly located within a nature reserve and are surrounded by low hills supplied with abundant atmospheric precipitation. Thus, with typical swamp-like conditions, the Daiyun Mountain peat is extremely sensitive to climatic changes, and offers an ideal site for studying regional climatic variability under a changing global climate. To date, the majority of Holocene pollen studies in Fujian Province have focused on coastal areas, flood plains and river deltas, while mountain areas have been somewhat neglected (Lan et al. 1986; Zheng 1991; Jin and Zheng 1993; Wu 1993; Wang et al. 1995; Chen et al. 1998a, b; Zheng et al. 2002; Zhi et al. 2003). Many studies have reconstructed vegetation and environmental changes (Liu and Qiu 1994; Qiu 2006; Xu et al. 2013; Huang et al. 2014; Yue et al. 2012, 2014) as well as the impact of human activities (Liu and Qiu 1994; Qiu 2006; Xu et al. 2013) in the monsoonal regions of southeastern China. Despite this, the climatic conditions, vegetation history and the impacts of human activities on Daiyun Mountain during the late Holocene remain poorly understood (Liu and Qiu 1994; Qiu 2006). Earlier studies in this region have relied on low-resolution sequences with poor chronological control (Liu and Qiu 1994; Qiu 2006). In contrast, the high-resolution multi-proxy record presented in this study offers a chronology based on precise accelerator mass spectrometry (AMS) radiocarbon (^{14}C) dating of a peat profile from Daiyun Mountain. Using this technique, we reconstruct the late Holocene vegetation and climate changes on a regional scale and analyze human impact on the vegetation and environment over the last millennium. Our study provides

additional data for research into global change, both in terms of tracing past conditions and modelling future scenarios.

Study area

The peatland selected for this study is located in a nature reserve on Daiyun Mountain, Fujian Province in south-eastern China. The Daiyun Mountain nature reserve ($25^{\circ}38'07''$ – $25^{\circ}43'40''\text{N}$, $118^{\circ}05'22''$ – $118^{\circ}20'15''\text{E}$) is located 40 km north of Dehua (Fig. 1). The Daiyun

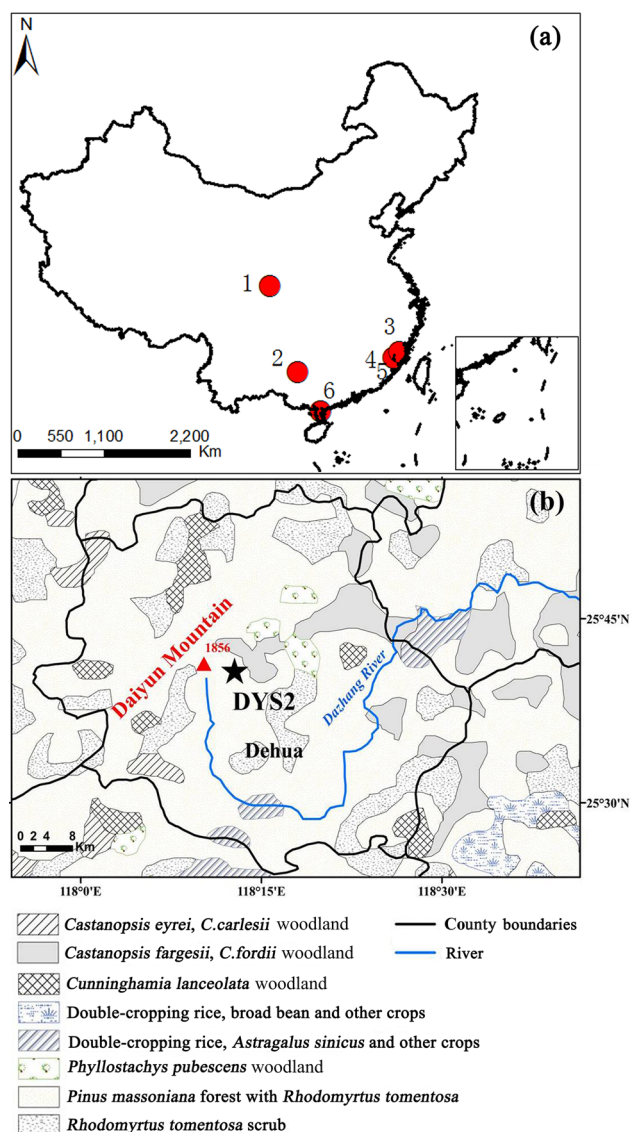


Fig. 1 Maps showing **a**, the geographical location of the study site and the modern vegetation of the study area: 1 Wanxiang cave (Zhang et al. 2008), 2 Dongge cave (Wang et al. 2005), 3 Pingnan peat (Yue et al. 2012), 4 Lianhuachi site (Qiu 2006), 5 Daiyun Mountain peat (DYS2), 6 Lake Huguangyan Marr (Yancheva et al. 2007; Wang et al. 2007), **b** modern vegetation of the DHS2 profile

Mountain range occupies the central part of this province, and comprises several peaks, including Daiyun (1,856 m a.s.l.), Jiuxian (1,655 m a.s.l.), Shiniu (1,781 m a.s.l.) and Zhiyundong (1,629 m a.s.l.). The mean annual temperature in the region is 15.6–19.5 °C and the mean annual precipitation is 1,700–1,900 mm. Daiyun Mountain is a subtropical oceanic climate under the strong influence of the southeast monsoon. Around 80 % of the annual precipitation falls during the rainy season between April and September (Lin 2002).

More than 90 % of the area is covered by subtropical evergreen broadleaf forests, mainly comprising evergreen trees such as *Quercus* and *Castanopsis* (Fig. 1). The vegetation community varies with altitude (Fig. 2a): below 500 m, the evergreen broadleaved forest is dominated by *Castanopsis tibetana*, *C. eyrei* and *C. fabri*, among others; from 500 to 1,000 m on the southern slopes of the mountain, broad-leaved evergreen forests, coniferous forests, and coniferous and broad-leaved mixed forests are dominated by species that include *Cunninghamia lanceolata*, *Pinus massoniana*, *Castanopsis fargesii*, *C. eyrei*, *Cyclobalanopsis myrsinifolia*, *Taxus chinensis* var. *mairei* and *Cryptomeria fortunei*; from 500 to 800 m on the northern slopes of the mountain, forests with some deciduous features are often interspersed with evergreen broadleaved forests, conifer forests, and conifer and broadleaved mixed forests. The species within the deciduous forests include *Quercus variabilis* and *Liquidambar formosana*; from 1,000 to 1,600 m on the southern slopes of the mountain and from 800 to 1,600 m on its northern slopes, vegetation is dominated by coniferous trees and wetland plants, which

mainly include *Cryptomeria fortunei*, *Tsuga longibracteata*, *Juncus effusus*, *Isachne globosa* and *Eleocharis tetraquetra*; above 1,600 m, the mountain summits are covered by broad-leaved evergreen shrubs dominated by *Rhododendron simsii*, *R. mariesii* and *Eurya saxicola*.

The peatland investigated in this study developed extensively during the Holocene. The total peat-covered area on Daiyun Mountain is approximately 100 m by 200 m, and the marshy environment allowed the accumulation of peat layers ranging from 1 to 3.2 m in thickness. Due to the area's poor drainage and the absence of any significant water bodies, the peatland has a stable sedimentary setting, with well-preserved continuous autochthonous sediments.

Materials and methods

Field sampling and dating

A 100 cm deep profile was excavated from the peatland on Daiyun Mountain in 2010 (25°40.040'N, 118°12.381'E; altitude, 1,579 m a.s.l.). Terrestrial plant macrofossils, peat (60–180 µm) and pollen samples were collected from four locations and dated using AMS (Table 1). Three samples were dated at the AMS Dating Laboratory of Beijing University, China, and one was dated by Beta Analytic, USA. Pollen extracts contained both terrestrial and aquatic pollen, in addition to other organic matter. While pollen dating can be problematic when aquatic plants are involved, we consider the use of pollen extraction for dating to be effective in reducing

Fig. 2 **a** Vegetation composition with altitude. **b** View of the peatland studied. **c** The vegetation landscape surrounding the DYS2 profile

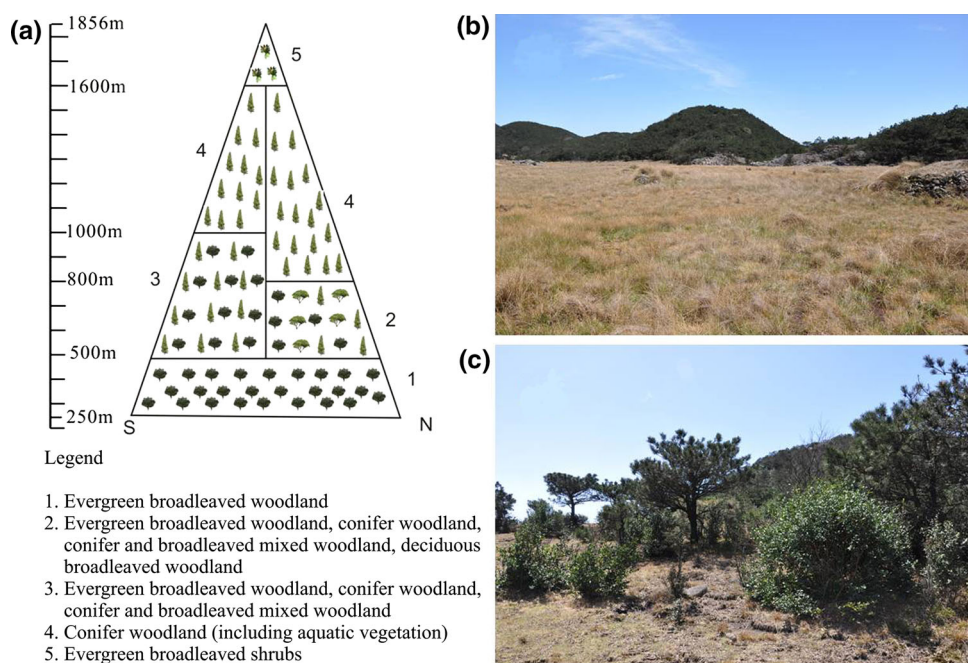


Table 1 AMS ^{14}C dates from DYS2 (this study) and the Lianhuachi site (Qiu 2006) from Fujian province, China

Lab. code	Sample ID	Depth (cm)	Material dated	^{14}C age (BP)	Age cal BP (1 σ)	Probability	Sedimentation (mm/a)	Reference
Beta-371397	DYSII-7	7	Pollen (extracted)	170 \pm 30	193 (168–218)	0.513	0.363	This paper
GZ4165	DYSII-57	57	Peat 60–180 μm	1,405 \pm 20	1,307 (1,294–1,320)	1	0.449	This paper
GZ4166	DYSII-77	77	Peat 60–180 μm	3,490 \pm 30	3,756 (3,736–3,777)	0.425	0.080	This paper
GZ4167	DYSII-100	100	Plant macrofossils	3,575 \pm 25	3,869 (3,840–3,898)	1	3.71	This paper
Beta-57823	CS90-4-8	35–40	Peat	1,240 \pm 100	1,168 \pm 100		0.322	Qiu 2006
Beta-47267	CS90-4-112	50–60	Peat	3,240 \pm 80	3,462 \pm 80		0.0617	Qiu 2006
Beta-37536	WS-1	90	Wood	3,930 \pm 60	4,406 \pm 60		0.0763	Qiu 2006

Beta, dates from Beta Analytic, Miami, USA; GZ, dates from AMS Dating Laboratory at Beijing University

the influence of old carbon to give more reliable ages, compared with bulk sample dating techniques. Many previous studies have indicated that pollen extraction from sediments is able to give more reliable stratigraphic ages (Zhou et al. 1997, 2005). All dates were calibrated to calendar years before present (0 = AD 1950) using CALIB Rev. 6.0.1 with the IntCal 09 calibration data set (Stuiver and Peimer 1993; Stuiver et al. 1998; Reimer et al. 2009). The age-depth model was established by fitting spline functions to the age control points using the Bacon model (Blaauw 2010); this task was carried out using the statistical software package R.

Pollen analysis

Forty-five samples were taken at 2 cm intervals for pollen analysis. Each sample contained 1–2 cm³ of peat material. Sample preparation followed the standard procedure, using 10 % HCl to remove carbonate and 10 % KOH to remove organic matter. Finally, pollen and charcoal were extracted using a heavy liquid (2.1 g ml⁻¹) composed of HBr, Zn and KI (500 ml: 120 g: 510 g) and sieved on a 7 μm mesh screen to obtain a higher concentration of pollen grains (Nakagawa et al. 1998). The concentrate was mounted in glycerol gel and *Lycopodium* tablets (27,637 grains/tablet) were added to each sample to enable calculation of the pollen concentration (Maher 1981). Each pollen sample was counted under a light microscope at $\times 400$ magnification and 1,000 \times was used for critical identifications. Pollen counts were usually >500 terrestrial pollen grains. Pollen identification was carried out using published pollen atlases by Wang et al. (1995) and Xi and Ning (1994), as well as the modern pollen collections of the laboratory. Pollen percentages of trees, shrubs and dry land herbs were calculated based on their pollen sums. The relative pollen percentages of wetland herbs and fern spores were then

established from the sums of all counted palynomorphs. The pollen diagram was plotted using Tilia 1.7.16 (Grimm 2011) and pollen assemblage zones were provided by stratigraphically constrained cluster analysis (CONISS) (Grimm 2011).

The charcoal record was prepared from pollen-slide charcoal counting in widely spaced profile samples. Micro-charcoals larger than 50 μm were counted in order to calculate their accumulation rates, as they may be used to reconstruct fire history, to indicate palaeovegetational and palaeoenvironmental changes and to mark any significant fire event in the study region (Patterson et al. 1987; Lv et al. 2002).

Geochemical analysis

The degree of peat humification, as indicated by fluctuations in absorbance, was determined following the alkaline extraction method described by Blackford and Chambers (1993). The analyses were performed using a personal computer-based 2102 UV–Visible spectrophotometer in the Soil Laboratory of the School of Geographic and Oceanographic Sciences, Nanjing University, China. The sediment core was sampled at 1 cm intervals and a total of 85 samples, each weighing 0.1 g, were used for the humification analysis.

Eighty-four subsamples weighing 2 g each were taken from depths of 3–86 cm in the sediment core for loss-on-ignition (LOI) analysis. Sequential combustion at 550 $^{\circ}\text{C}$ was used to estimate the organic matter content (Dean 1974).

Data analysis

Numerical analyses were conducted using only those taxa that occurred in at least three samples with a percentage of

>1 %. A total of 30 pollen taxa were used and the analysis was carried out using CANOCO v.4.52 (Ter Braak and Smilauer 2003). Detrended correspondence analysis (DCA) was used to determine whether linear or unimodal based techniques should be employed in the subsequent ordination analysis. The length of the gradient was 1.363 standard deviation (SD) units, which was less than 3. Therefore, a principal component analysis (PCA) (Birks and Gordon 1985; Birks 1998) was performed to analyze the pollen assemblages using inter-species correlations and square-root transformations of pollen percentages.

Results

Lithology and radiocarbon dates

Four stratigraphic units are identified, and are presented in Fig. 3. Unit 1 (uppermost 32 cm) consists of yellow–brown peat, with an organic matter content of 24.28 %. Unit 2 (32–61 cm) is distinguished by its black colour and high organic matter content of around 40 %; this banded peat section is dark with highly humified peat layers (Fig. 3). Unit 3 (61–90 cm) consists of brown peat with an organic matter content of 22.92 %. Finally, Unit 4 (90–100 cm) consists of sand and gravel.

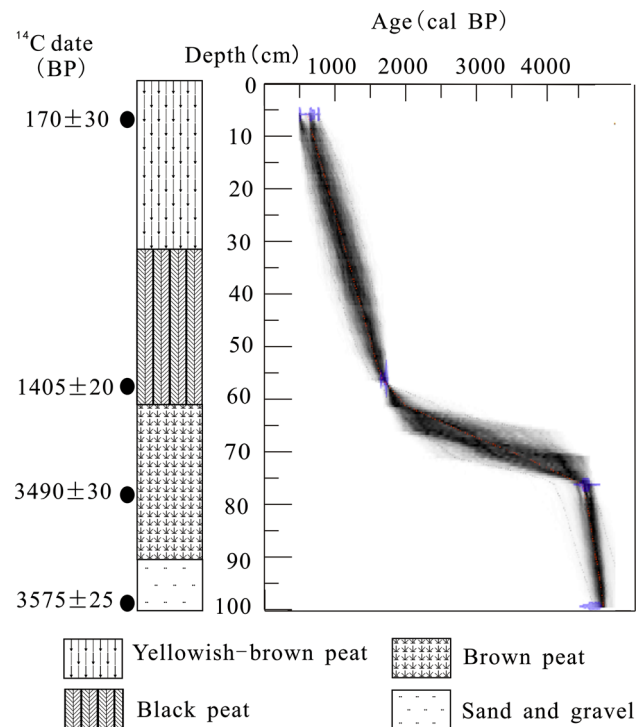


Fig. 3 Age/depth model based on four calibrated AMS ^{14}C dates (see Table 1 for details). The chronology for the section 0–7 cm is difficult to read in the chronology curve, but consisted of a linear function for this short section

consists of sand and gravel with the lowest amount of organic matter.

The four calculated dates (in calendar ages) were used to construct the age–depth model, which was established by fitting spline functions to the age control points using the Bacon model (Blaauw 2010) (Fig. 3). This chronology indicates that the peat profile spans the last 4,460 years. Therefore, the temporal sampling resolution for the lithological analysis is 45 years for each contiguous 1 cm interval, while each centimetre represents 90 years of the fossil pollen record. Ages based on this model are used in the discussion section below. The lower unit (77–100 cm) was found to have a sedimentation rate of 3.71 mm a^{-1} ; the upper units (0–7, 7–57 cm) had similar rates of 0.363 mm a^{-1} and 0.449 mm a^{-1} , respectively. However, the sedimentation rate of the middle unit was considerably lower, at 0.080 mm a^{-1} . Comparing the lithologies and peat accumulation rates at our study site with those at the nearby Lianhuachi site ($25^{\circ}40'15''\text{N}$, $118^{\circ}11'12''\text{E}$; 1,550 m a.s.l.) reported by Qiu (2006), we can see that the peat depths in both areas are the same (approximately 90–100 cm), and that the accumulation rates in the upper units (approximately 0–60 cm) of the two sites are high, while those of the lower units are low (Table 1). The correspondence of our results with those from pollen stratigraphy at Lianhuachi confirms the reliability of the chronology constructed in this study.

Fossil pollen data

A total of 96 pollen and spore types were identified in the 45 samples, including 57 trees and shrubs, 33 herbs, six ferns and three types of moss and algal palynomorphs. The identified pollen taxa spanned coniferous, tropical, subtropical and temperate vegetation types. The coniferous taxa mainly included *Pinus*, *Picea*, *Tsuga*, Podocarpaceae and Taxodiaceae. The tropical and subtropical broad-leaved taxa mainly include *Castanopsis* (including *Lithocarpus*), *Ilex* and evergreen *Quercus* (including *Cyclobalanopsis*). The temperate broad-leaved taxa include *Alnus*, *Carpinus*, *Betula*, *Pterocarya*, *Fagus*, deciduous *Quercus*, Ericaceae, *Corylus*, *Carya*, *Juglans*, *Acer*, *Tilia* and Rosaceae. The main dry land herbaceous taxa are Poaceae, Asteraceae, *Artemisia*, Lamiaceae, *Humulus*, Brassicaceae, Fabaceae, Apiaceae, *Thalictrum* and Campanulaceae. The main wetland herbs are Cyperaceae, Liliaceae, *Polygonum*, Ranunculaceae, Potamogetonaceae, *Myriophyllum* and *Typha*. The identified spores mainly consist of Polypodiaceae, Hymenophyllaceae, *Pteris*, *Selaginella*, Parkeriaceae and trilete spores. Two pollen zones, each with two subzones, were identified (Figs. 4, 5).

Zone 1 (91–48 cm depth; 4,350–1,000 cal BP): pollen percentages are dominated by evergreen *Quercus* (ranging

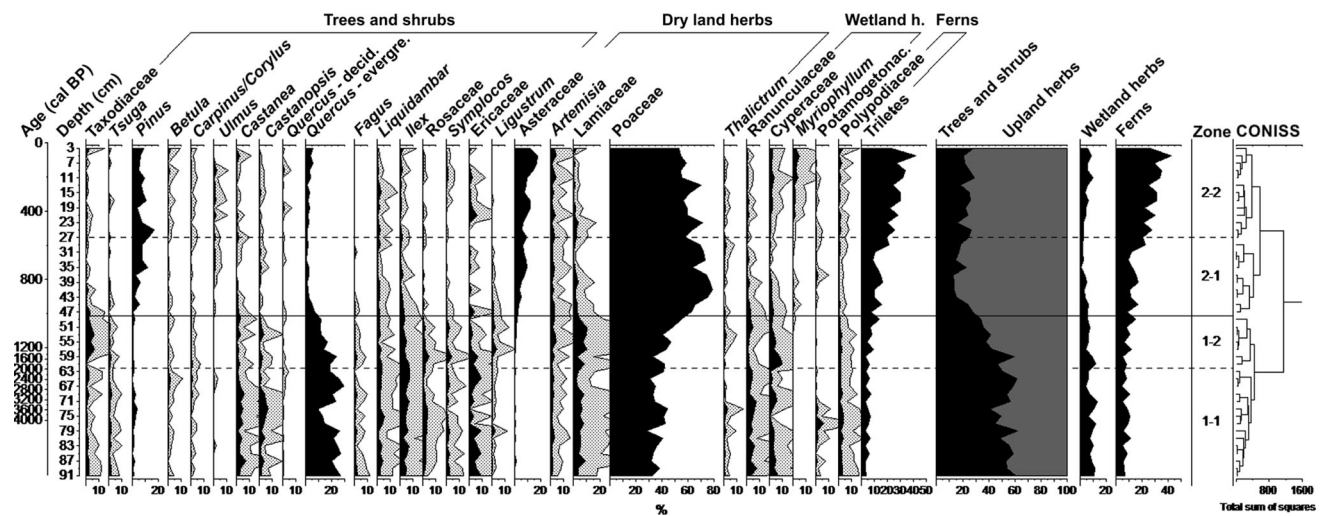


Fig. 4 Pollen percentage diagram of the DYS2 profile with the 28 main taxa and the four main pollen zones obtained from a constrained cluster analysis. The pollen sum used is “trees and shrubs (AP) + dry

land herbs (NAP)”, except for wetland herbs and ferns, which use the pollen sum “trees and shrubs + dry land herbs + wetland herbs + ferns”; shadow is $\times 5$ magnification

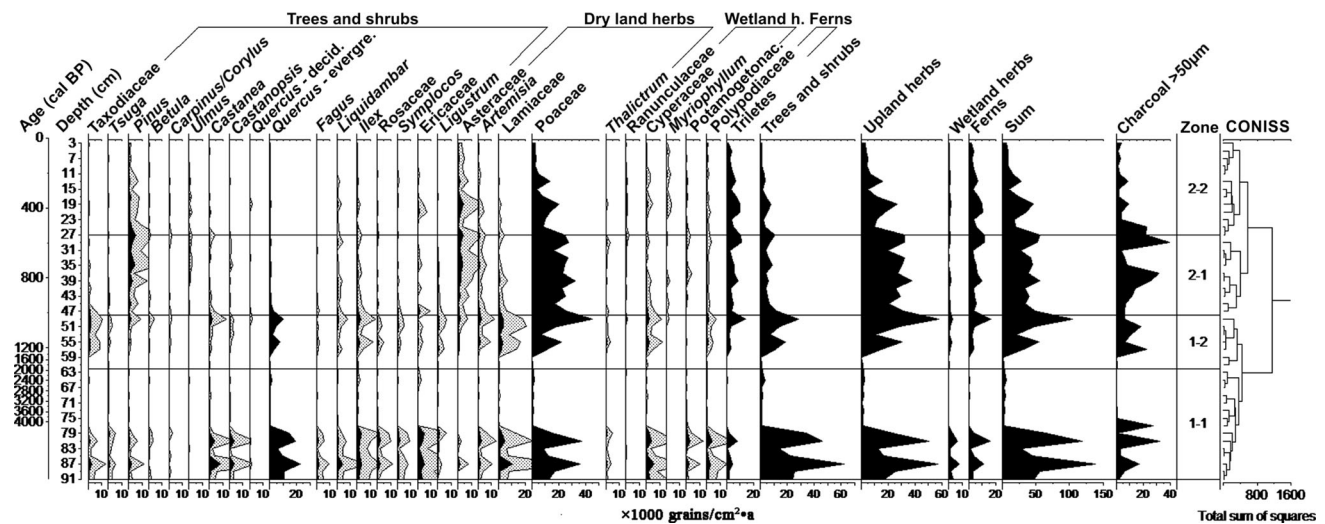


Fig. 5 PARs from the DYS2 profile with the 28 main taxa and the four main pollen zones obtained from a constrained cluster analysis; shadow is $\times 5$ magnification

from 9.7 to 26.9 %, mean of 19.7 %) and *Castanopsis* (mean of 2.3 %), with some *Castanea*, *Liquidambar*, *Ilex* and *Ericaceae*. The pollen percentage of dry land herbs fluctuates between 37.9 and 66.2 % with *Poaceae* as the major taxon (mean 38.8 %). In addition, there is a relatively high percentage of wetland herbs (mean 7.3 %) and a low percentage of fern spores (mean 8.6 %). The pollen accumulation rate (PAR) fluctuates between 632 and 138,420 grains $\text{cm}^{-2} \text{a}^{-1}$. This zone is characterized by the highest abundance of evergreen *Quercus* but the lowest abundance of herbaceous pollen. The zone can be divided into two subzones: Subzone 1-1 (91–62 cm depth; 4,350–1,550 cal BP) contains the highest percentage of

evergreen *Quercus* and the lowest *Poaceae* percentage within the entire profile. In addition, the percentages of *Castanopsis*, *Castanea*, *Liquidambar*, *Ilex* and *Cyperaceae* are relatively high, whereas the percentages of *Asteraceae* and *Artemisia* are low. The PAR is low, at 35,093 grains $\text{cm}^{-2} \text{a}^{-1}$. Subzone 1-2 (62–48 cm depth, 1,550–1,000 cal BP) is marked by a sharp increase in *Poaceae* and a slight decrease in evergreen *Quercus*. However, pollen assemblages are still dominated by evergreen *Quercus*. The PAR is 37,770 grains $\text{cm}^{-2} \text{a}^{-1}$.

Zone 2 (48–0 cm depth; 1,000–0 cal BP): This zone is characterized by the highest percentage of dry land herbs (mean 78.78 %); however, it has the lowest percentage and

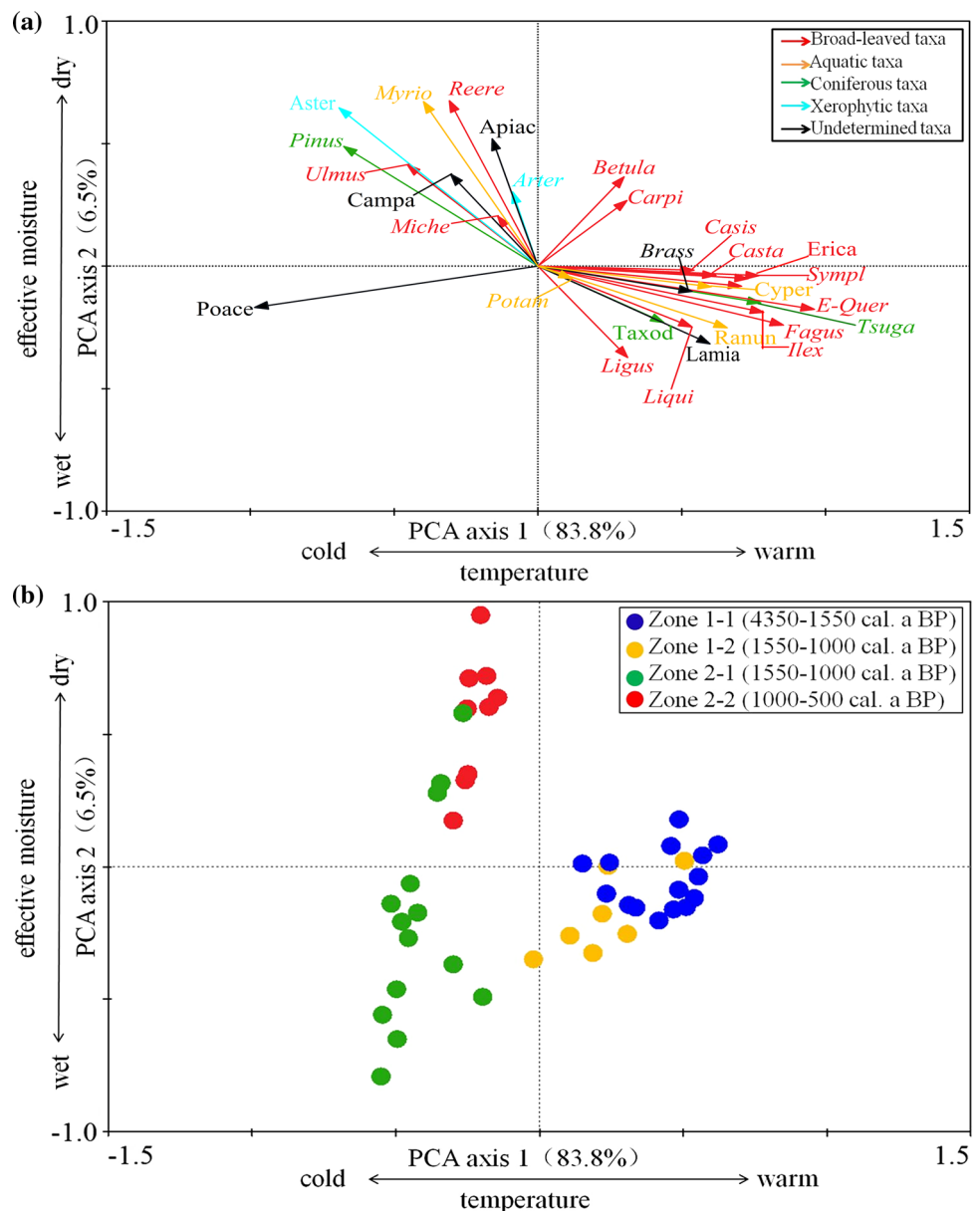
PAR of trees and shrubs (mean 21.22 %, 4,837 grains $\text{cm}^{-2} \text{a}^{-1}$). In addition, there is a relatively low percentage of wetland herbs (mean 4.4 %) and a high percentage of fern spores (mean 22 %). Poaceae, *Pinus* and Asteraceae increase markedly, while evergreen *Quercus* shows a notable decrease. This zone can also be divided into two subzones. Subzone 2-1 (48–27 cm depth; 1,000–550 cal BP) is marked by the highest percentage of dry land herbs and the lowest percentage and PAR of trees and shrubs. *Pinus*, Poaceae and Asteraceae increase markedly, while evergreen *Quercus*, *Castanopsis*, *Castanea*, *Liquidambar* and *Ilex* decrease considerably. There is a relatively low content of wetland herbs and a high content of trilete spores. Subzone 2-2 (27–0 cm depth; 550–0 cal BP) also

contains a high percentage and high PAR of dry land herbs and a low percentage and PAR of trees and shrubs. The percentages and PARs of Poaceae, *Pinus* and Asteraceae are high, but slightly less than in Subzone 2-1, whereas the percentages and PARs of evergreen *Quercus*, *Castanopsis*, *Castanea*, *Liquidambar* and *Ilex* are low. There is a relatively low content of wetland herbs and a high content of trilete spores.

PCA results

PCA results based on pollen samples and pollen taxa reflect the characteristics of the pollen assemblages and effectively summarize the main vegetation changes (Fig. 6).

Fig. 6 PCA results for fossil pollen data from DYS2 (Campa: Campanulaceae; *Miche*: *Michelia*; Poace: Poaceae; *Ligus*: *Ligustrum*; *Myrio*: *Myriophyllum*; *Apiac*: Apiaceae; *Arter*: *Artemisia*; *Potam*: Potamogetonaceae; *Aster*: Asteraceae; *Ranun*: Ranunculaceae; *Carpi*: *Carpinus*; *Brass*: Brassicaceae; *Reere*: *Reevesia*; *Taxod*: Taxodiaceae; *Liqui*: *Liquidambar*; *E-Quer*: evergreen *Quercus*; *Casis*: *Castanopsis*; *Casta*: *Castanea*; *Erica*: Ericaceae; *Lamia*: Lamiaceae; *Sympl*: *Symplocos*; *Rosac*: Rosaceae; *Cyper*: Cyperaceae)



The first two principal components (Axis 1 and Axis 2) capture 83.8 and 6.5 % of the total variance in the data set. PCA Axis 1 (PCA-1) mainly reflects relative changes between warm temperature taxa such as evergreen *Quercus*, *Ilex*, *Fagus* and *Tsuga*, as shown on the right side of Fig. 6a, and cold-tolerant taxa such as Poaceae and Asteraceae, as shown on the left side of the figure. PCA Axis 2 (PCA-2) separates the mesic taxa such as Ranunculaceae from the drought-resistant ones such as *Artemisia*. Based on the ecological affinities of individual taxa, it is evident that Axis 1 therefore represents changes in summer temperature, because pollen assemblages typically reflect vegetation conditions during the flowering seasons. In contrast, Axis 2 represents changes in effective moisture. Four clusters can be identified on the basis of the PCA scores along the first two axes, as shown in Fig. 6b; these correspond to the pollen assemblage zones defined by CONISS (Grimm 2011) (Figs. 4, 5).

Humification and LOI

Figure 7 shows that both the mean degree of humification (17.52 %) and LOI (26.45 %) are low during the period 4,350–1,000 cal BP. Organic matter varies between 25 and 41.18 % during 1,000–550 cal BP. After 550 cal BP, the

mean LOI is relatively lower (22.72 %). Additionally, the degree of humification shows a decreasing trend from 1,000 cal BP to 550 cal BP, with the lowest mean value (10.2 %) found between 550 cal BP and the present.

Discussion

Vegetation history and climate since 4,350 cal BP

Knowledge of the size of the pollen catchment is essential for interpreting pollen assemblages in terms of pollen source areas. Typically, the boundary for local pollen ranges between 20 and 30 m within the sedimentary basin. The presence of local pollen is therefore a reflection of the surrounding vegetation and has important implications for the reconstruction and succession of local vegetation (Bradshaw 1981; Jacobson and Bradshaw 1981; Prentice 1985; Xu and Zhang 2013). In contrast, regional pollen refers to that pollen which covers a range of 100–2,000 m within the sedimentary basin and is important for studies into vegetation reconstruction and climate change (Nielsen and Sugita 2005; Wang and Herzschuh 2011; Xu and Zhang 2013). The peat bog investigated in this study is approximately 100 m wide and 200 m long, and has

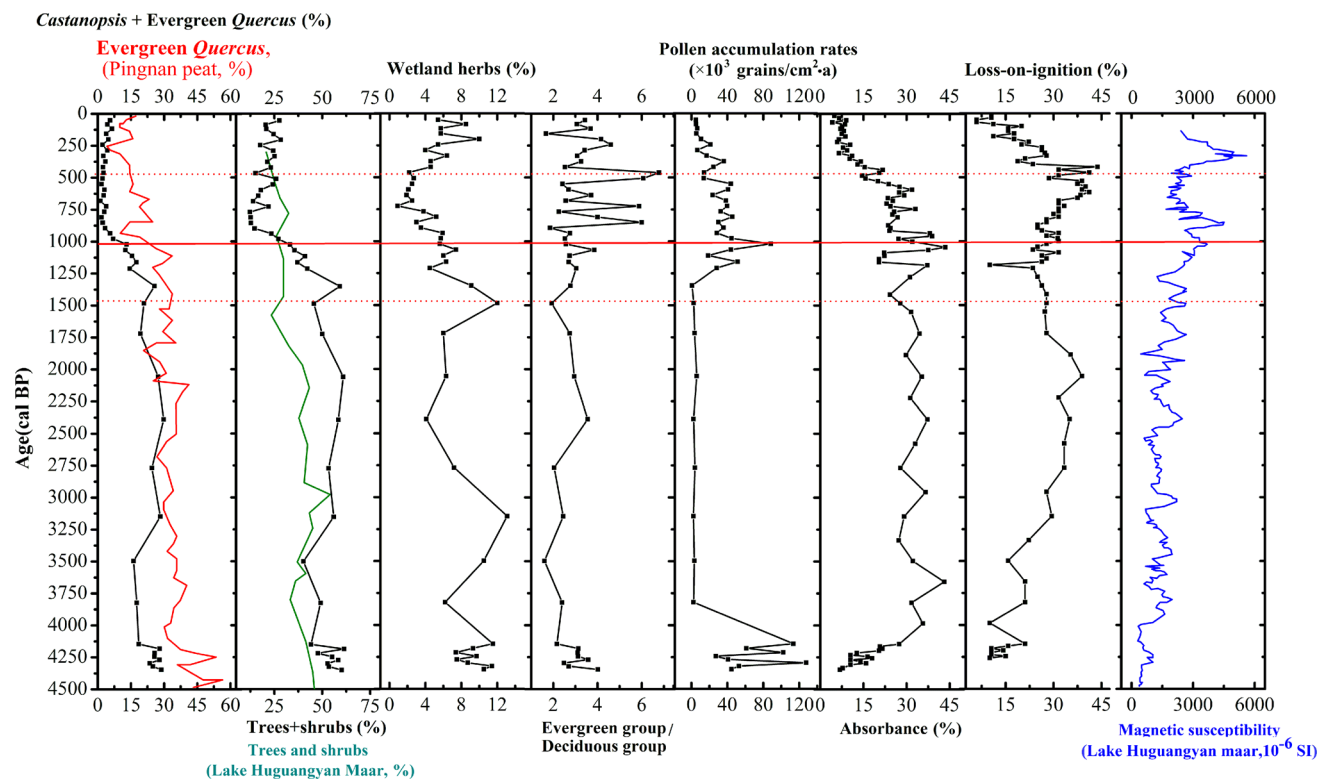


Fig. 7 Comparison of multiproxy data in the DYS2 profile and pollen percentages (trees + shrubs) from Lake Huguangyan Maar (Wang et al. 2007), of evergreen *Quercus* from the Pingnan peat (Yue

et al. 2012) and magnetic susceptibility from Lake Huguangyan Maar (Yancheva et al. 2007)

accumulated a 1.0 m thick peat layer. As this peatland is enclosed without the presence of a river, we can consider the sources of pollen to be both local and regional. This allows a high resolution reconstruction of vegetation history and climate changes in the Daiyun Mountain region during the late Holocene.

4,350 to 1,550 cal BP

This pollen zone was characterized by high pollen percentages of wetland herbs, trees and shrubs, as well as a small pollen percentage of dry land herbs. Taxa typical of the warm subtropics, such as evergreen *Quercus*, *Castanea*, *Castanopsis*, *Ilex* and *Liquidambar*, dominate this zone. Poaceae and Lamiaceae are the major contributors to the dry land herbs, while Cyperaceae and Ranunculaceae are the major wetland herbs. The vegetation mainly comprised evergreen forests dominated by broad-leaved trees, indicating a warm and wet climate at this time. Previous studies have also found high pollen percentages of *Castanopsis* and evergreen *Quercus* in the Fuzhou basin (Yue et al. 2014) and the Pingnan peat (Yue et al. 2012) during 4,000–1,000 cal BP, supporting the interpretation of a warm climate during this period. Additionally, results from Lake Huguangyan Maar (Fig. 7; Wang et al. 2007; Yancheva et al. 2007; Wu et al. 2012), indicating low magnetic susceptibility (also see Fig. 7) and high total organic carbon, support the interpretation of a warm climate during 4,350–1,550 cal BP.

1,550 to 1,000 cal BP

The pollen diagram shows a decrease in the pollen percentage from trees and shrubs, but increased pollen percentage and PAR from dry land herbs. Evergreen *Quercus*, *Castanopsis*, *Castanea*, *Ilex* and *Liquidambar* decline significantly, while Poaceae and Asteraceae increase. Additionally, wetland herbs, predominantly Cyperaceae and Ranunculaceae, show a significant decline. The vegetation at this time was therefore dominated by evergreen forests, suggesting a warm and wet climate, similar to the previous stage. Wang et al. (2007) also reported high relative pollen abundance of trees and shrubs from Lake Huguangyan Maar in southern subtropical China, while Yancheva et al. (2007) reported low magnetic susceptibility in the same lake. Both of these results support our interpretation of a warm and wet climate during this period.

1,000 to 550 cal BP

This zone is characterized by a high pollen percentage and PAR of dry land herbs, and low pollen percentages and

PARs of trees, shrubs and wetland herbs. The vegetation mainly comprised degraded forests at this time, with a sharp decline seen in trees and shrubs, corresponding to an abundance of well-developed herbs, indicating ecological succession due to disturbance of the vegetation. A significant change in the vegetation occurred after 1,000 cal BP, with a sharp reduction of evergreen trees including *Quercus*, *Castanopsis*, *Castanea*, *Ilex* and *Liquidambar*, and an increase in Poaceae and Asteraceae. LOI, absorbance and the ratio of evergreen to deciduous groups are high, whereas the wetland herbs are scarce during this period, suggesting that a cool and dry climate prevailed in the Daiyun Mountain region at this time (Fig. 7). Most of the late Holocene pollen records from southeastern China consistently show a gradual decline in evergreen forests, such as those dominated by evergreen *Quercus*, after 1,000 cal BP (Liu and Qiu 1994; Qiu 2006; Yue et al. 2014). It is believed that the climate in southeastern China became cooler during the late Holocene, probably associated with a weakening of the summer monsoon.

550 cal BP to present

The pollen percentage and PAR of trees and shrubs are low, whereas dry land herbs, largely composed of Poaceae and Asteraceae, are high at this time. The vegetation had become increasingly degraded, as indicated by the sharply decreased pollen percentage and PAR from trees and shrubs and plentiful pollen from herbs. LOI, absorbance and the ratio of evergreen to deciduous groups are low whereas wetland herbs are abundant (Fig. 7), suggesting a wet and cold climate since 550 cal BP. A previous study by Wang et al. (2007) reported a similar low abundance of tree and shrub pollen and Yancheva et al. (2007) documented low magnetic susceptibility from Lake Huguangyan Maar in south China. Additionally, a number of pollen records also show a gradual decline in trees, especially evergreen forests, since 550 cal BP in Fujian Province (Liu and Qiu 1994; Qiu 2006; Yue et al. 2014). All of these studies suggest a similar climate to that inferred from our results.

Overall, vegetation was dominated by evergreen forests mainly composed of broadleaf trees during 4,350–1,000 cal BP, suggesting a warm climate at this time. The pollen percentage and PAR of trees and shrubs sharply decrease after 1,000 cal BP, indicating a cooling climate. Pollen records from the SZY core in Fujian also show an abrupt decrease in evergreen broadleaved tree pollen around 2,600 cal BP, indicating a cooling climate, driven by the weakening East Asian monsoon (Yue et al. 2012). We find that most of the late Holocene pollen records consistently show a gradual decline in evergreen forests, such as those dominated by evergreen *Quercus*, after 2,000 cal BP (Liu and Qiu 1994; Qiu 2006; Yue et al. 2014). It is therefore believed that the

climate in southern China became cooler during the late Holocene, probably associated with a weakening summer monsoon. Oxygen isotopes measured in Dongge Cave exhibit negative values, indicating a weak Asian monsoon during the late Holocene (Wang et al. 2005). Similar patterns in oxygen isotope values have also been reported from Shanbao Cave further north (Shao et al. 2006; Wang et al. 2008). Together, these results support our interpretations of the varying climate conditions in our study area during the late Holocene. In addition to this, Xu et al. (2013) suggested that human activities have influenced the vegetation changes in the mountainous regions of Fujian Province of south-eastern China during the last 1,300 years. In the section below, we further investigate human impacts on vegetation and the environment since 1,000 cal BP.

Climate events: the warm period from AD 670 to 960, the MWP and the LIA

In our study, we suggest that the chronology may not be sufficiently robust for discussion of climate events, as they have not been accurately dated. However, by comparing the lithologies and peat accumulation rates from our study site with those from the nearby Lianhuachi site (25°40'15"N, 118°11'12"E; 1,550 m a.s.l.) from Qiu (2006), we can be more certain of the reliability of the chronology constructed in this study. Thus, we can identify the timings of climate events with some degree of uncertainty through the reconstruction of late Holocene vegetation and climate change, and therefore consider that the timings of climate events described here are reliable.

Both LOI and humification are good proxies for past climate and environment conditions (Aaby 1976; Zhang et al. 1998; Borgmark and Schoning 2006; Daley and Barber 2012). High LOI and humification suggest a dry climate, while low LOI and humification indicate a wet climate (Aaby 1976; Zhang et al. 1998; Zhou et al. 2004; Borgmark 2005; Borgmark and Schoning 2006; Ma et al. 2009). In this study, we analyzed the peat humification, LOI, pollen accumulation rates and the ratio of evergreen groups to deciduous groups in our study area, and compared the results with the winter half-year mean temperature change over the last 2,000 years in eastern China (Ge et al. 2002), in addition to the $\delta^{18}\text{O}$ record from Wanxiang Cave (Fig. 8; Zhang et al. 2008). While the differences between summer temperatures in the north and south of China are small, a significant difference can be seen in winter temperatures. As a result, temperature changes caused by varying solar radiation are more obvious during the winter under the background of climate change. Thus, we consider it reasonable to compare our data to the temperature changes in the winter half-years. Overall, the changes recorded in the six curves are largely consistent,

since two warm periods and a cold period can be identified. For AD 670–960, the pollen accumulation rates peak, suggesting a warm period, which can be confirmed by the winter half-year mean temperature record in eastern China. Additional evidence in the form of negative $\delta^{18}\text{O}$ at Wanxiang Cave and low LOI and absorbance further suggest that the climate was warm and wet from AD 670 to 960. This stage corresponds to the third warm period (AD 600–1000) in the climate evolution of eastern China over the past 5,000 years as suggested by Zhu (1973). However, the Daiyun Mountain peat records reveal that this warm period began later and ended earlier than the times established by Zhu (1973) and that the event was shorter and cooler than the medieval warm period (MWP). We suggest that the area was possibly cooled by the winter monsoon.

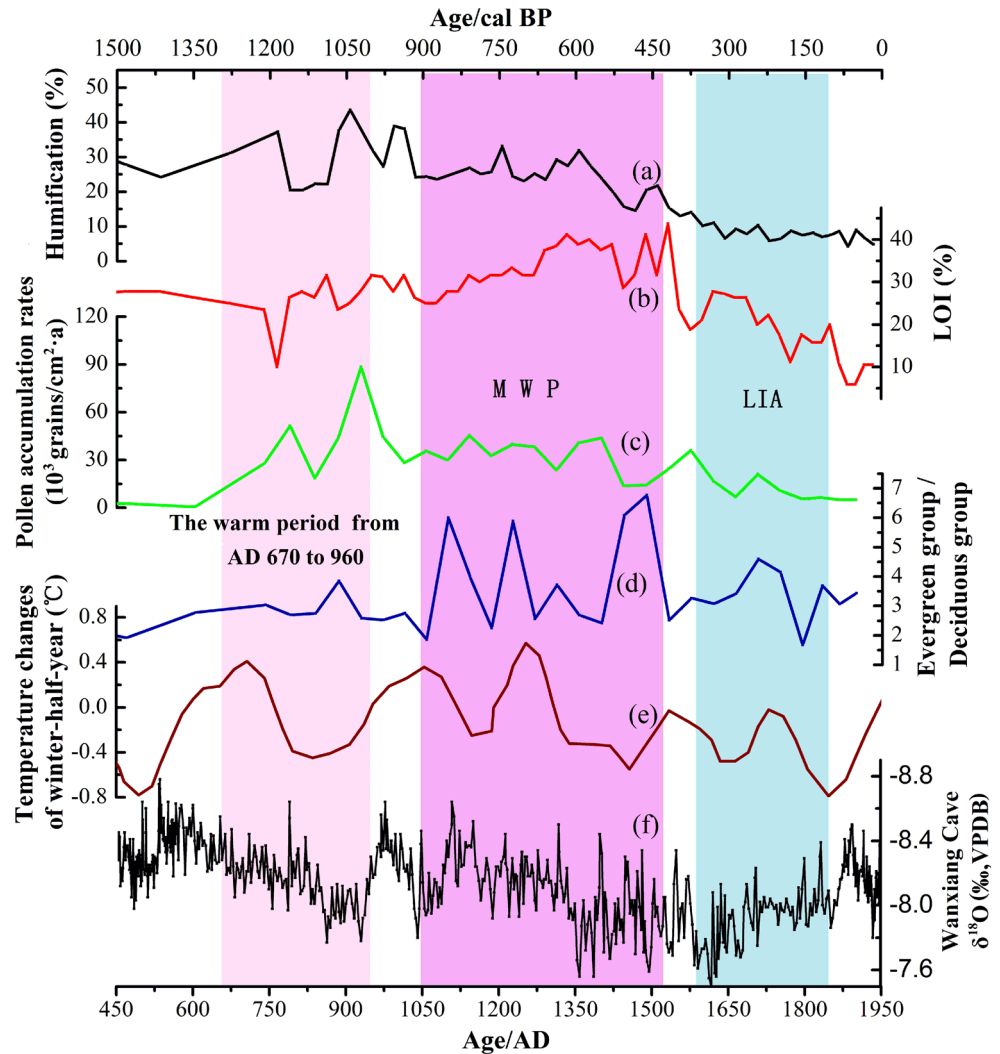
Many studies have attempted to reconstruct the climate changes during the MWP, however the beginning and end of this event remain controversial (Adhikari and Kumon 2001; Mann and Jones 2003; Yang et al. 2003; Driese et al. 2004; Pla and Catalan 2005; Matul et al. 2007; Yang et al. 2007). Nevertheless, the period from AD 800 to 1400 is generally considered to cover the MWP time span (Zuo and Jin 2009; Wang 2010). Thus, the climate fluctuations during the MWP can be recognized in our peat record. Based on our results, the MWP occurred around AD 1050–1520, with relatively a dry and warm climate compared with the warm period from AD 670 to 960. The ratio of evergreen to deciduous pollen was also higher during the MWP, suggesting a warmer climate, while the higher absorbance and LOI indicate dry conditions at this time. The evergreen to deciduous pollen ratio was high during AD 1060–1280 and 1430–1520, indicating that the climate was relatively warm during these two stages; these correspond to the two temperature peaks, with a 150 year long relatively cool period between. This pattern is considered broadly consistent with the main features of the climate fluctuations during the MWP.

From AD 1580 to 1850, both the evergreen to deciduous pollen ratio and pollen accumulation rates are low, corresponding to the low temperatures of the reconstructed winter half-year temperature record in eastern China. This suggests that the climate during this period, which corresponds to the LIA, was cold. In addition, low LOI and absorbance and negative $\delta^{18}\text{O}$ values from Wanxiang Cave suggest a wet climate at this time. As such, the LIA may have corresponded to the cold periods of the Ming and Qing dynasties (Zhu 1973).

Human impact on vegetation and environment since 1,000 cal BP

Since 1,000 cal BP, the abundance of evergreen trees such as *Castanopsis*, *Ilex* and evergreen *Quercus*, and deciduous broad-leaf trees and shrubs such as Rosaceae and

Fig. 8 Overview chart illustrating *a* peat humification in the DYS2 profile, *b* the loss on ignition in the DYS2 profile, *c* PARs of the DYS2 profile, *d* the ratio of evergreen groups to deciduous groups, *e* temperature changes of winter half-years in eastern China (Ge et al. 2002), *f* $\delta^{18}\text{O}$ record from Wanxiang Cave (Zhang et al. 2008)



Ericaceae, decreased in our pollen data. Both human activities and climate change could have been the cause of such substantial changes in trees and shrubs. Human activities tend to result in the decline of selective woody plant taxa in small patches in the same region (Li et al. 2008). In contrast, a reduction of climate-sensitive trees and shrubs over large areas tends to be driven by climatic change (Li et al. 2008). In our study area, therefore, the declining numbers of evergreen trees and deciduous broadleaved trees and shrubs may have been caused by the use of these as building materials or fuel. In addition, our data suggest that secondary pine forests and grasses increased significantly at the same time, suggesting the beginning of farming in the region. According to Liu and Qiu (1994) and Qiu (2006), who have also reconstructed vegetation change in Fujian Province, the collapse of primeval vegetation communities occurred around 1,200 cal BP. This was represented by an abrupt decline in *Castanopsis* and evergreen *Quercus* pollen and a noticeable

increase in *Pinus* and Poaceae pollen percentages. Additionally, the pollen record from Pingnan peat (Xu et al. 2013) also indicated a gradual decrease in *Castanopsis* and evergreen *Quercus* pollen, accompanied by a continuous increase in Poaceae pollen since approximately 800 cal BP; this pattern may be interpreted as reflecting the spread of rice cultivation. A large number of pollen records from lake sediments and soil profiles are also characterized by a reduction in arboreal pollen, such as *Pinus*, evergreen *Quercus* and *Cyclobalanopsis*, in parallel with a rise in herbaceous pollen, such as *Artemisia*, Poaceae and Chenopodiaceae, as a result of human influence during the late Holocene in east-central, southern, and northeastern China (Tarasov et al. 2006; Chen et al. 2009; Cao et al. 2010; Li et al. 2014).

A high concentration of charcoal usually indicates abundant fire activity (Chen 1990) and previous studies have suggested that the concentration of charcoal (>50 μm) is a convincing indicator of regional or local fire

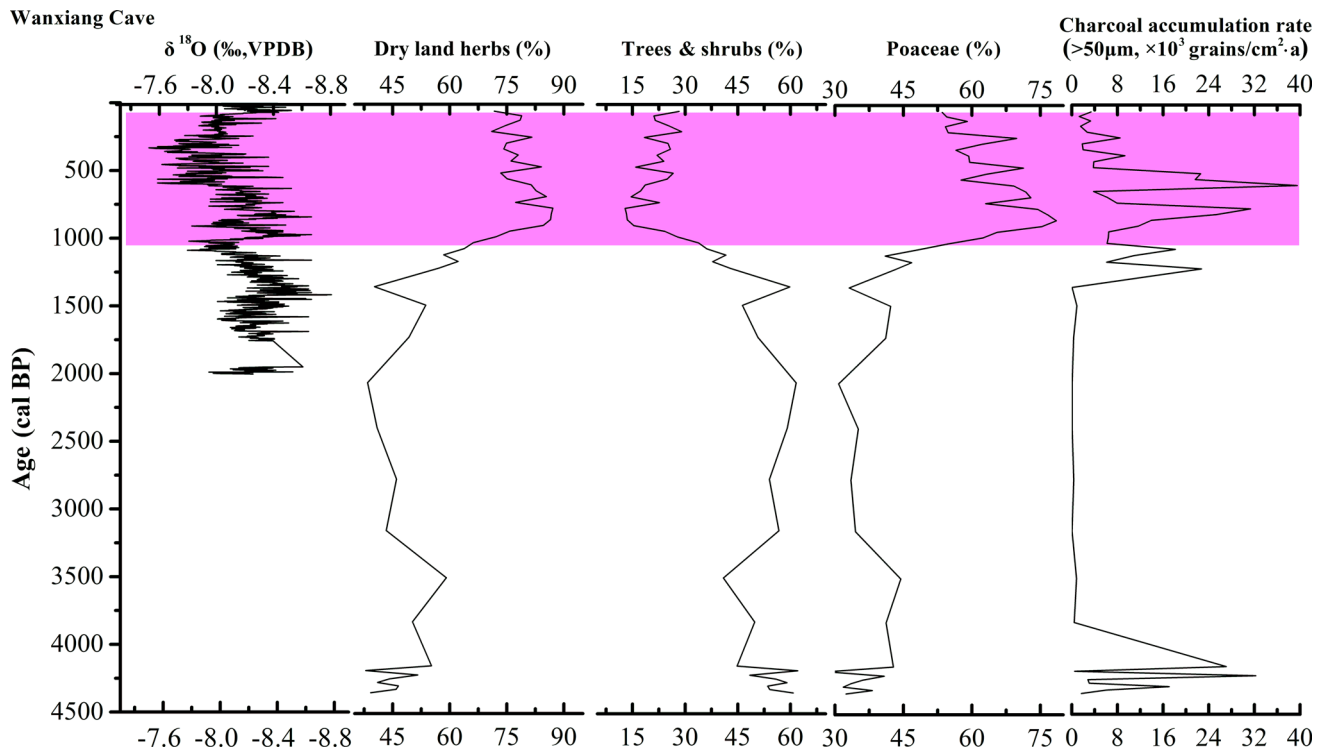


Fig. 9 Map showing changes in dry land herbs, trees and shrubs, Poaceae pollen, charcoal concentration (>50 μm), and the $\delta^{18}\text{O}$ record from Dongge Cave (Wang et al. 2005) during the last 4,350 years (red shading highlights the influence of human activities)

activity (Minckley et al. 2007; Sadori and Giardini 2007; Egli et al. 2012; Zhao et al. 2012). Combined with pollen data, charcoal can be used to reconstruct fire history, palaeovegetation and palaeoenvironmental changes (Patterson et al. 1987; Lv et al. 2002). In this context, charcoal can not only indicate the long-term fire regime and climate changes, but also the dynamic intensity of human activities (Jiang et al. 2008; Marquer et al. 2008). The pollen percentages of dry land herbs, trees and shrubs, and Poaceae were compared with charcoal (>50 μm) accumulation rates and $\delta^{18}\text{O}$ from the Wanxiang cave (Fig. 9; Zhang et al. 2008). From this, we found that the charcoal accumulation rates can precisely indicate the frequency and intensity of fires, which are closely linked with human activities in our study area. Figure 8 shows positive $\delta^{18}\text{O}$, suggesting a weaker monsoon since 1,000 cal BP, corresponding to a low pollen percentage of trees and shrubs. Moreover, Poaceae pollen and the charcoal accumulation rates (>50 μm) increase and reach their peaks during this period, which suggests increased human activities since 1,000 cal BP.

The population of Quanzhou City, which falls within our broad study area, increased rapidly during the Sui and Tang dynasties (Chen and Chen 2011). According to historical documents, many people moved to Quanzhou in the early Tang dynasty, resulting in a great expansion of farming in the surrounding regions (Chen and Chen 2011). The population doubled during the Song and Yuan dynasties

(Chen and Chen 2011) and the increasing population had major impacts on the vegetation and the environment.

The natural vegetation in our study area is mostly coniferous and broadleaved mixed forest and broadleaved forest with some pine forest. It is known that the forest of Dehua County became an important source of fuel for the development of the ceramics industry from the Song dynasty onwards (Chen and Chen 2011). Increasing charcoal accumulation rate may therefore be linked to the clearance of trees for fuel. Liu and Qiu (1994) reported similar vegetation changes and speculated that human activities were the cause of vegetation degradation. Additionally, several environmental archaeology studies into the Fujian shell mound have suggested that people abandoned aquatic resources in the region after 2,000 cal BP, due to the expansion of paddy rice culture (Cai 1998; Qu and Chen 2010). Therefore, the sharp decrease of woody plants identified here may conceivably be linked to human activities.

Conclusions

In this study, a 4,350 year history of vegetation and climate changes was reconstructed based on pollen, LOI and humification records in peat sediments. We conclude:

1. Vegetation was dominated by evergreen forests, mainly composed of broadleaved trees during the period 4,350–1,000 cal BP, indicating a warm and wet climate. From 1,000 to 550 cal BP, a cool but dry climate can be inferred from the decreased pollen percentages and PARs of trees, shrubs and wetland herbs. The pollen percentage and PAR of dry land herbs, as well as LOI, increased between 1,000 and 550 cal BP. Finally, a higher pollen abundance of dry land and wetland herbs, along with low pollen percentage and PAR of trees and shrubs, low absorbance and LOI, suggest a cooler but wetter climate after 550 cal BP. In the future, further analysis of modern pollen assemblages is necessary, to permit a quantitative reconstruction of palaeoclimate based on the pollen database of East Asia.
2. Climate events of the warm period from AD 670 to 960, the MWP (AD 1050–1520) and the LIA (AD 1580–1850) can be identified from our records, with the climate of each period being characteristically warm and wet, warm and dry, and cold and wet, respectively. In this study, the chronology of these climate events may not be adequately robust, as there are as yet no accurate dates for them. However, we can identify the period in which the climate events took place from reconstructions of late Holocene vegetation and climate change.
3. Human activities may have had a very significant impact on the natural vegetation during the last 1 ka. Pollen and charcoal signals indicate strong human influence since 1,000 cal BP, which may be linked to the development of the porcelain industry in Dehua County and the rapidly increasing population within Quanzhou City in our study region.

Acknowledgments We are grateful to the staff of the Daiyun Mountain National Nature Reserve for access permission and Wei Shi, Feixue Feng and Dang Li for assistance during the field work. We thank the editor and two anonymous reviewers for their helpful comments and suggestions that improved the manuscript. This research was jointly funded by the National Natural Science Foundation of China (NSFC, No. 41371202), the Strategic Priority Research Program of the Chinese Academy of Sciences (XDA05120704), 973 Program under Grant (No.2015CB953800) and the open-ended fund (SKLLQG1313) from the State Key Laboratory of Loess and Quaternary Geology, Institute of Earth Environment of the China Academy of Sciences.

References

- Aaby B (1976) Cyclic climatic variations in climate over the past 5500 yr reflected in raised bogs. *Nature* 263:281–284
- Adhikari DP, Kumon F (2001) Climatic changes during the past 1,300 years as deduced from the sediments of Lake Nakatsuna, central Japan. *Limnology* 2:157–168

- Birks HJB (1998) D.G. Frey and E.S. Deevey review 1: numerical tools in palaeolimnology-progress, potentialities and problems. *J Paleolimnol* 20:307–332
- Birks HJB, Gordon AD (1985) Numerical methods in quaternary pollen analysis. Academic Press, London
- Blaauw M (2010) Methods and code for “classical” age modeling of radiocarbon sequences. *Quat Geochronol* 5:512–518
- Blackford JJ, Chambers FM (1993) Determining the degree of peat decomposition for peat-based palaeoclimatic studies. *Int Peat* 5:7–24
- Borgmark A (2005) Holocene climate variability and periodicities in south-central Sweden, as interpreted from peat humification analysis. *Holocene* 15:387–395
- Borgmark A, Schoning K (2006) A comparative study of peat proxies from two eastern central Swedish bogs and their relation to meteorological data. *J Quat Sci* 21:109–114
- Bradshaw RHW (1981) Quantitative reconstruction of local woodland vegetation using pollen analysis from a small basin in Norfolk, England. *J Ecol* 69:941–955
- Cai BQ (1998) The living environment and resource development in coastal of Fujian from the shell mound site. *J Xiamen Univ* 3:106–111 (In Chinese)
- Cao XY, Xu QH, Jing ZC, Tang JG, Li YC, Tian F (2010) Holocene climate change and human impacts implied from the pollen records in Anyang, central China. *Quat Int* 227:3–9
- Chen YS (1990) Forest fire in early Holocene forest changes at Lake Barrine, Australia. *Acta Bot Sin* 32:69–75 (In Chinese with English abstract)
- Chen JZ, Chen DL (2011) Dehua porcelain. Culture and Art Press, Beijing
- Chen WR, Lan DZ, Chen CH (1998a) Late Quaternary data and sea level changes in estuarine plain of the Jiulong River. *Acta Oceanol Sin* 20:65–72 (In Chinese with English abstract)
- Chen WR, Lan DZ, Chen CH, Yu YF (1998b) Sporopollen assemblages and climatic-environmental changes in Jiulongjiang Estuarine Plain during Late Quaternary. *J Oceanogr Taiwan Strait* 17:34–42 (In Chinese with English abstract)
- Chen W, Wang WM, Dai XR (2009) Holocene vegetation history with implications of human impact in the Lake Chaohu area, Anhui Province, East China. *Veget Hist Archaeobot* 18:137–146
- Chen JH, Chen FH, Feng S, Huang W, Liu JB, Zhou AF (2015) Hydroclimatic changes in China and surroundings during the medieval climate anomaly and little ice age: spatial patterns and possible mechanisms. *Quat Sci Rev* 107:98–111
- Chu GQ, Liu JQ, Sun Q, Lu HY, Gu ZY, Wang WY, Liu TS (2002) The ‘Mediaeval Warm Period’ drought recorded in Lake Huguangyan, tropical South China. *Holocene* 12:511–516
- Cichon M, Niedzielski P (2015) Dirt road: a geomorphological and geochemical record of Late-Holocene human activity in the catchment of Lake Radacz (Central Pomerania, Poland). *Quat Int* 370:145–158
- Cronin TM, Dwyer GS, Kamiya T, Schwede S, Willard DA (2003) Medieval Warm Period, Little Ice Age and 20th century temperature variability from Chesapeake Bay. *Glob Planet Chang* 36:17–29
- Daley TJ, Barber KE (2012) Multi-proxy Holocene palaeoclimate records from Walton Moss, northern England and Dosenmoor, northern Germany, assessed using three statistical approaches. *Quat Int* 268:111–127
- Dean WE (1974) Determination of carbonate and organic matter in calcareous sediments and sedimentary rocks by loss on ignition: comparison with other methods. *J Sedim Petrol* 44:242–248
- Driese SG, Ashley GM, Li ZH, Hoverc VC, Owen RB (2004) Possible Late Holocene equatorial palaeoclimate record based upon soils spanning the Medieval Warm Period and Little Ice

- Age, Lobo Plain, Kenya. *Palaeogeogr Palaeoclimatol Palaeoecol* 213:231–250
- Egli M, Mastrolonardo G, Seiler R, Raimondi S, Favilli F, Crimi V, Krebs R, Cherubini P, Certini G (2012) Charcoal and stable soil organic matter as indicators of fire frequency, climate and past vegetation in volcanic soils of Mt. Etna, Sicily. *Catena* 88:14–26
- Faust D, Zielhofer C, Escudero RB, Del Olmo FD (2004) High-resolution fluvial record of Late Holocene geomorphic change in northern Tunisia: climatic or human impact? *Quat Sci Rev* 23:1,757–1,775
- Ge QS, Zheng JY, Fang XQ, Man ZM, Zhang XQ, Zhang PY, Wang WQ (2002) Temperature changes of winter-half-year in eastern China during the past 2,000 years. *Quat Sci* 2:166–173 (**In Chinese with English abstract**)
- Grimm E (2011) Tilia and Tiliagraph software 1.7.16. Illinois State Museum, Springfield
- Huang KY, Zheng Z, Liao WB, Cao LL, Zheng YW, Zhang H, Zhu GQ, Zhang Z, Cheddadi R (2014) Reconstructing Late Holocene vegetation and fire histories in monsoonal region of southeastern China. *Palaeogeogr Palaeoclimatol Palaeoecol* 393:102–110
- Jacobson GL, Bradshaw RHW (1981) The selection of sites for palaeovegetational studies. *Quat Res* 16:80–96
- Jiang WY, Leroy SAG, Ogle N, Chu GQ, Wang L, Liu JQ (2008) Natural and anthropogenic forest fires recorded in the Holocene pollen record from a Jinchuan peat bog, northeastern China. *Palaeogeogr Palaeoclimatol Palaeoecol* 261:47–57
- Jin DS, Zheng F (1993) Palaeoclimate in the coastal area of central Fujian, 120,000 years BP. *Geol Fujian* 12:218–227 (**In Chinese with English abstract**)
- Lan DZ, Yu YF, Chen CH, Xie ZT (1986) Preliminary study on Late Pleistocene transgression and Holocene sea-level fluctuation in Fuzhou Basin. *Mar Geol Quat Geol* 6:103–111 (**In Chinese with English abstract**)
- Li YY, Zhou LP, Cui HT (2008) Pollen indicators of human activity. *Chin Sci Bull* 53:1,281–1,293
- Li JY, Zhao Y, Xu QH, Zheng Z, Lv HY, Luo YL, Li YC, Li CH, Seppä H (2014) Human influence as a potential source of bias in pollen-based quantitative climate reconstructions. *Quat Sci Rev* 99:112–121
- Lin P (2002) A compressive report of Daiyun Mountain Natural Reserve in Fujian Province. Xiamen University Press, Fujian
- Liu KB, Qiu HL (1994) Late Holocene pollen records of vegetational changes in China: climate or human disturbance? *Terr Atmos Ocean Sci* 5:393–410
- Lv J, Wang YF, Li CS (2002) Fossil charcoal and ancient forest fire. *J Palaeogeogr* 4:71–76 (**In Chinese with English abstract**)
- Ma CM, Zhu C, Zheng ZG, Yin Q, Zhao ZP (2009) Climate changes in East China since the Late-glacial inferred from high-resolution mountain peat humification records. *Sci China Ser D* 52:118–131
- Maher LJ (1981) Statistics for microfossil concentration measurements employing samples spiked with marker grains. *Rev Palaeobot Palynol* 32:153–191
- Mann ME, Jones PD (2003) Global surface temperatures over the past two millennia. *Geophys Res Lett* 30:18–20
- Marquer L, Pomel S, Abichou A, Schulz E, Kaniewski D, Campo EV (2008) Late Holocene resolution palaeoclimatic reconstruction inferred from Sebkhah Mhabeul, southeast Tunisia. *Quat Res* 70:240–250
- Matul AG, Khusid TA, Mukhina VV, Chekhovskaya MP, Safarova SA (2007) Recent and late Holocene environments on the southeastern shelf of the Laptev Sea as inferred from microfossil data. *Oceanology* 47:80–90
- Minckley T, Whitlock C, Bartlein P (2007) Vegetation, fire, and climate history of the northwestern Great Basin during the last 14,000 years. *Quat Sci Rev* 26:2167–2184
- Nakagawa T, Brugiapaglia E, Digerfeldt G, Reille M, De Beaulieu JL, Yasuda Y (1998) Dense-media separation as a more efficient pollen extraction method for use with organic sediment samples: comparison with the conventional method. *Boreas* 25:15–24
- Nielsen AB, Sugita S (2005) Estimating relevant source area of pollen for small Danish lakes around AD 1800. *Holocene* 15:1006–1020
- Patterson WA, Edwards KJ, Maquire DJ (1987) Microscopic charcoal as a fossil indicator fire. *Quat Sci Rev* 6:3–23
- Pla S, Catalan J (2005) Chrysophyte cysts from lake sediments reveal the sub-millennial winter/spring climate variability in the northwestern Mediterranean region throughout the Holocene. *Clim Dyn* 24:263–278
- Prentice IC (1985) Pollen representation, source area, and basin size: toward a unified theory of pollen analysis. *Quat Res* 23:76–86
- Qiu HL (2006) A 4000 year pollen record of vegetation change from the subtropical mountains of Fujian Province, China. *J Subtrop Resour Environ* 1:11–23
- Qu XL, Chen ZY (2010) The reasons of shell mound sites disappeared by comparison of the Shandong Peninsula and the coastal Fujian. *Fujian Fair* 2:6–11
- Quamar MF, Chauhan MS (2014) Signals of Medieval Warm Period and Little Ice Age from southwestern Madhya Pradesh (India): a pollen-inferred Late-Holocene vegetation and climate change. *Quat Int* 325:74–82
- Reimer PJ, Baillie MGL, Bard E et al (2009) INTCAL 09 and MARINE09 radiocarbon age calibration curves, 0–50,000 years cal BP. *Radiocarbon* 51:1111–1150
- Sadori L, Giardini M (2007) Charcoal analysis, a method to study vegetation and climate of the Holocene: the case of Lago di Pergusa (Sicily, Italy). *Geobios* 40:173–180
- Sadori L, Giardini M, Gliozzi E, Mazzini I, Sulpizio R, Van Welden A, Zanchetta G (2015) Vegetation, climate and environmental history of the last 4500 years at lake Shkodra (Albania/Montenegro). *Holocene* 25:435–444
- Shao XH, Wang YJ, Cheng H, Kong XG, Wu JY, Lawrence ER (2006) Long-term trend and abrupt events of the Holocene Asian monsoon inferred from a stalagmite $\delta^{18}O$ record from Shennongjia in Central China. *Chin Sci Bull* 51:80–86
- Stuiver M, Reimer PJ (1993) Extended ^{14}C data base and revised Calib 3.0 ^{14}C age calibration program. *Radiocarbon* 35:215–230
- Stuiver M, Reimer PJ, Bard E et al (1998) Intcal 98 Radiocarbon age calibration 24000–0 cal BP. *Radiocarbon* 40:1,041–1,083
- Tan LC, Cai YJ, Cheng H, An ZS, Edwards RL (2009) Summer monsoon precipitation variations in central China over the past 750 years derived from a high resolution absolute-dated stalagmite. *Palaeogeogr Palaeoclimatol Palaeoecol* 280:432–439
- Tarasov PE, Jin GY, Wagner M (2006) Mid-Holocene environmental and human dynamics in northeastern China reconstructed from pollen and archaeological data. *Palaeogeogr Palaeoclimatol Palaeoecol* 241:284–300
- Ter Braak CJF, Smilauer P (2003) Canoco for Windows v. 4.52. Biometris, Wageningen
- Tian ZH, Han YM, Cao JJ, Huang CC, An ZS (2015) Holocene wildfire history and human activity from high-resolution charcoal and elemental black carbon records in the Guanzhong Basin of the Loess Plateau, China. *Quat Sci Rev* 109:76–87
- Turner TE, Swindles GT, Roucoux KH (2014) Late Holocene ecohydrological and carbon dynamics of a UK raised bog: impact of human activity and climate change. *Quat Sci Rev* 84:65–85
- Van der Linden M, Barke J, Vickery E, Charman DJ, Van Geel B (2008) Late Holocene human impact and climate change recorded in a North Swedish peat deposit. *Palaeogeogr Palaeoclimatol Palaeoecol* 258:1–27
- Viau AE, Ladd M, Gajewski K (2012) The climate of North America during the past 2,000 years reconstructed from pollen data. *Glob Planet Chang* 84–85:75–83

- Wang SW (2010) Medieval warm period and little ice age. *Adv Clim Chang Res* 6(5):388–390 **(In Chinese)**
- Wang YB, Herzschuh U (2011) Reassessment of Holocene vegetation change on the upper Tibetan Plateau using the pollen-based REVEALS model. *Rev Palaeobot Palynol* 168:31–40
- Wang FX, Qian NF, Zhang YL (1995a) Pollen flora of China. Science Press, Beijing
- Wang KF, Lu JJ, Zheng YL (1995b) Late Quaternary pollen-diatom assemblages along Fujian seashore and their palaeoenvironmental implication. *Acta Micropalaeontol Sin* 12:388–397 **(In Chinese with English abstract)**
- Wang YJ, Cheng H, Edwards RL, He YQ, Kong XG, An ZS, Wu JY, Kelly MJ, Dykoski CA, Li XD (2005) The Holocene Asian monsoon: links to solar changes and North Atlantic climate. *Science* 308:854–857
- Wang SY, Lu HY, Liu JQ, Negendank Jörg FW (2007) The early Holocene optimum inferred from a high-resolution pollen record of Huguangyan Maar Lake in southern China. *Chin Sci Bull* 52:2,829–2,836
- Wang YJ, Cheng H, Edwards RL et al (2008) Millennial- and orbital-scale changes in the East Asian monsoon over the past 224,000 years. *Nature* 451:1,090–1,093
- Wu XZ (1993) Holocene sporopollen assemblage in Mawei, Fuzhou City and their geological significance. *Geol Fujian* 4:292–299 **(In Chinese with English abstract)**
- Wu XD, Zhang ZH, Xu XM, Shen J (2012) Asian summer monsoonal variations during the Holocene revealed by Huguangyan Maar lake sediment record. *Palaeogeogr Palaeoclimatol Palaeoecol* 323–325:13–21
- Xi YZ, Ning JZ (1994) Pollen morphology of arid and semi-arid regions of China. *Yushan Biol* 11:119–191 **(In Chinese with English abstract)**
- Xu QH, Zhang SR (2013) Advance in pollen source area. *Adv Earth Sci* 28:968–975 **(In Chinese with English abstract)**
- Xu JX, Zheng Z, Huang KY, Yue YY, Li J, Chase BM, Ledru MP, Carré M, Cheddadi R (2013) Impacts of human activities on ecosystems during the past 1,300 years in Pingnan area of Fujian Province, China. *Quat Int* 286:29–35
- Yancheva G, Nowaczyk NR, Mingram J et al (2007) Influence of the intertropical convergence zone on the East Asian monsoon. *Nature* 445:74–77
- Yang B, Bräuning A, Shi YF (2003) Late Holocene temperature fluctuations on the Tibetan Plateau. *Quat Sci Rev* 22:2,335–2,344
- Yang B, Bräuning A, Yao TD, Davis ME (2007) Correlation between the oxygen isotope record from Dasuopu ice core and the Asian Southwest Monsoon during the last millennium. *Quat Sci Rev* 26:1,810–1,817
- Yue YF, Zheng Z, Huang KY, Chevalier M, Chase BM, Carré M, Ledru MP, Cheddadi R (2012) A continuous record of vegetation and climate change over the past 50,000 years in the Fujian Province of eastern subtropical China. *Palaeogeogr Palaeoclimatol Palaeoecol* 365–366:115–123
- Yue YF, Zheng Z, Rolett BV, Ma T, Chen C, Huang KY, Lin GW, Zhu GQ, Cheddadi R (2014) Holocene vegetation, environment and anthropogenic influence in the Fuzhou Basin, southeast China. *J Asian Earth Sci* 99:85–94
- Zeng Y, Chen JG, Zhu ZJ, Li J, Wang JF, Wan GJ (2012) The wet Little Ice Age recorded by sediments in Huguangyan Lake, tropical South China. *Quat Int* 263:55–62
- Zhang JH, Kong ZC, Du NQ (1998) The response of Loss-on-ignition range to past climate and environment in Beijing. *Acta Ecol Sin* 18:343–347 **(In Chinese with English abstract)**
- Zhang PZ, Cheng H, Edwards RL, Chen FH, Wang YJ, Yang XL, Liu J, Tan M, Wang XF, Liu JH (2008) A test of climate, sun, and culture relationships from an 1,810-year Chinese cave record. *Science* 322:940–942
- Zhang Y, Liu XT, Lin QX, Gao CY, Wang J, Wang GP (2014) Vegetation and climate change over the past 800 years in the monsoon margin of northeastern China reconstructed from n-alkanes from the Great Hinggan Mountain ombrotrophic peat bog. *Org Geochem* 76:128–135
- Zhao ZY, Yuan DX, Shi SQ, Luo LD (2012) MIS3b vegetation and climate changes based on pollen and charcoal on Qianxi Plateau. *Acta Ecol Sin* 32:4,811–4,818 **(In Chinese with English abstract)**
- Zheng Z (1991) Pollen flora and palaeoclimate of the Chaoshan Plain during the last 50,000 years. *Acta Micropalaeontol Sin* 8:461–480 **(In Chinese with English abstract)**
- Zheng RZ, Xu XW, Zhu JF, Ji FJ, Huang ZL, Li JP (2002) Division of Late Quaternary strata and analysis of palaeoenvironment in Fuzhou basin. *Seismol Geol* 24:503–513 **(In Chinese with English abstract)**
- Zhi CY, Wang KF, Lan DZ, Chen CH, Zheng YL (2003) Study on the relationship between diatom assemblage and palaeoenvironment of the Late Quaternary in the Taiwan Channel and Xinmen Island. *Acta Micropalaeontol Sin* 20:244–252 **(In Chinese with English abstract)**
- Zhou WJ, Donahue D, Jull AJ (1997) Radiocarbon AMS dating of pollen concentrated from eolian sediments. *Radiocarbon* 39:19–26
- Zhou WJ, Yu XF, Jull AJT, Burr G, Xiao JY, Lu XF, Xian F (2004) High-resolution evidence from southern China of an early Holocene optimum and a mid-Holocene dry event during the past 18000 years. *Quat Res* 62:39–48
- Zhou WJ, Xie SC, Meyers PA, Zheng YH (2005) Reconstruction of Late glacial and Holocene climate evolution in southern China from geolipids and pollen in the Dingnan peat sequence. *Org Geochem* 36:1,272–1,284
- Zhu KZ (1973) Preliminary studies of climate change in China nearly five thousand years. *Chin Sci Bull* 2:168–189 **(In Chinese)**
- Zuo XX, Jin HL (2009) An overview of studies on Medieval Warm Period. *J Desert Res* 1:136–142 **(In Chinese with English abstract)**